

# Developmental adaptations to increased fetal nutrient demand in mouse genetic models of Igf2-mediated overgrowth

Emily Angiolini,<sup>\*,†,§</sup> Phillip M. Coan,<sup>‡</sup> Ionel Sandovici,<sup>†,‡,§</sup> O. H. Iwajomo,<sup>\*</sup> Gerrard Peck,<sup>†,§</sup> Graham J. Burton,<sup>‡</sup> Colin P. Sibley,<sup>||</sup> Wolf Reik,<sup>\*,‡</sup> Abigail L. Fowden,<sup>‡</sup> and Miguel Constância<sup>†,‡,§,1</sup>

\*Laboratory of Developmental Genetics and Imprinting, The Babraham Institute, Babraham Research Campus, Cambridge, UK; †Metabolic Research Laboratories, Department of Obstetrics and Gynaecology, and ‡Centre for Trophoblast Research, Department of Physiology, Development, and Neuroscience, University of Cambridge, Cambridge, UK; §National Institute of Health Research Cambridge Biomedical Research Centre, Cambridge, UK; and ||Maternal and Fetal Health Research Centre, School of Biomedicine, Manchester Academic Health Sciences Centre, University of Manchester, St. Mary's Hospital, Manchester, UK

**ABSTRACT** The healthy development of the fetus depends on an optimal balance between fetal genetic drive for growth and the maternal ability to provide nutrients through the placenta. Nothing is known about fetal-placental signaling in response to increased fetal demand in the situation of overgrowth. Here, we examined this question using the *H19*<sup>Δ13</sup> mouse model, shown previously to result in elevated levels of *Igf2*. Fetal and placental weights in *H19*<sup>Δ13</sup> were increased by 23% and 45%, respectively, at E19, when compared with wild-type mice. Unexpectedly, we found that disproportionately large *H19*<sup>Δ13</sup> placentas transport 20–35% less (per gram placenta) glucose and system A amino acids and have similar reductions in passive permeability, despite a significantly greater surface area for nutrient exchange and theoretical diffusion capacity compared with wild-type mice. Expression of key transporter genes *Slc2a3* and *Slc38a4* was reduced by ~20%. Decreasing the overgrowth of the *H19*<sup>Δ13</sup> placenta by genetically reducing levels of *Igf2P0* resulted in up-regulation of system A activity and maintenance of fetal overgrowth. Our results provide direct evidence that large placentas can modify their nutrient transfer capacity to regulate fetal nutrient acquisition. Our findings are indicative of fetal-placental signaling mechanisms that limit total demand for maternal nutrients.—Angiolini, E., Coan, P. M., Sandovici, I., Iwajomo, O. H., Peck, G., Burton, G. J., Sibley, C. P., Reik, W., Fowden, A. L., Constância, M. Developmental adaptations to increased fetal nutrient demand in mouse genetic models of Igf2-mediated overgrowth. *FASEB J.* 25, 1737–1745 (2011). [www.fasebj.org](http://www.fasebj.org)

**Key Words:** genomic imprinting • insulin-like growth factor • H19 • placenta

FETAL OVERGROWTH IS ASSOCIATED with an increased risk of complications both for the mother and infant at birth (1, 2). High birthweight in human populations is

also associated with development of metabolic syndrome in childhood, as well as with an increased risk of obesity and metabolic disease in later life (3, 4). Large-for-gestational-age (LGA) infants are becoming more common in many parts of the world as a result of improved maternal nutrition, higher prepregnancy BMI, and an increasing prevalence of gestational diabetes (4, 5). While it is clear that the maternal environment plays an important role in determining fetal size, intrauterine growth is determined ultimately by the fetal genetic drive for growth (demand for nutrients) and the ability of the placenta to supply oxygen and nutrients to the fetus. Interactions between the fetal genome and maternal environment controlling fetal nutrient acquisition are thought to occur, in part, *via* adaptations in placental phenotype (6–8), although little is known about the mechanisms involved in the fetal-placental signaling of nutrient demand.

Imprinted genes are important regulators of the balance between supply and demand systems that are crucial to fine-tune mammalian growth (9–11). The distinctive features of imprinted genes are their mono-allelic parental-specific expression, and their selective roles in key mammalian physiological pathways related to maternal resource acquisition (12, 13). Recent studies of murine knockouts for imprinted genes have shown that the capacity of the placenta to supply nutrients to the fetus varies according to fetal demand (14–17). The small *Igf2*-deficient P0 placenta compensates for its growth deficiency by up-regulating nutrient

<sup>1</sup> Correspondence: Metabolic Research Laboratories, Department of Obstetrics and Gynaecology, University of Cambridge, The Rosie Hospital, Robinson Way, Cambridge CB2 0SW, UK. E-mail: [jmasmc2@cam.ac.uk](mailto:jmasmc2@cam.ac.uk)

doi: 10.1096/fj.10-175273

This article includes supplemental data. Please visit <http://www.fasebj.org> to obtain this information.

transporters in response to a normal fetal growth demand (14, 15). These placentas are highly “efficient” because they are able to support normal fetal growth until near term, when fetal growth restriction finally ensues. When the fetal demand is reduced, as seen in the total *Igf2* knockout, this up-regulation is no longer observed, which strongly suggests that fetal demand influences placental phenotype (15). Similar adaptations in the nutrient transfer capacity of the placenta are seen when fetal demand exceeds the placental supply of nutrients during natural variations in placental growth (18). So far, these studies have been focused on models in which the potential for fetal growth is compromised by placental growth restriction. However, nothing is known about fetal-placental signaling in response to genetically determined overgrowth, despite the importance of these mechanisms to fully understanding the causes and consequences of growth-related complications of human pregnancy.

Here, we investigate placental adaptations in response to increased fetal growth demands in the imprinted *H19*<sup>Δ13</sup> mouse model of overgrowth (19). *H19* is a noncoding RNA, which is exclusively expressed from the maternal allele. Deletion of 13 kb, including the *H19* gene and the *H19/Igf2*-imprinting control region IC1 (also known as *H19* DMD), when transmitted maternally, leads to increased levels of *Igf2* and fetal overgrowth (19, 20). Excess of *Igf2* caused by disruption of IC1 has been implicated in the etiology of the overgrowth disorder Beckwith-Wiedemann syndrome (BWS), which is characterized by macroglossia, organomegaly, predisposition to embryonal tumors, and endocrine dysfunction (10, 21). Placentomegaly is commonly observed in mothers carrying BWS fetuses (22). In the *H19*<sup>Δ13</sup> mouse model, placental weight is increased as a result of the doubling of all *Igf2* transcripts, including the placental-specific P0 transcript (20, 23). The *H19*<sup>Δ13</sup> placentas are more overgrown than the fetus (20) and relatively “inefficient” as they produce fewer grams of fetus per gram of placenta compared to wild type (WT). We set out to test the hypothesis that *H19*<sup>Δ13</sup> placentas are less efficient because nutrient transfer to the fetus is reduced, perhaps in response to mechanisms that avoid excess drainage of maternal resources that might otherwise compromise fetal viability and future reproductive success.

## MATERIALS AND METHODS

### Mice

*H19*<sup>Δ13</sup> and *Igf2P0* mutant mice were generated as described previously (19, 24), and bred into an inbred C57BL6/J line for >10 generations. In experiments involving the single *H19*<sup>Δ13</sup> knockout, the mutant alleles were transmitted by a heterozygous mother, giving the genotypes *H19*<sup>Δ13</sup> (-/+ ) and WT (+/+); further information in Supplemental Fig. S1). In experiments involving crosses between *H19*<sup>Δ13</sup> and *Igf2P0* mice, the mutant alleles were transmitted by a homozygous *H19*<sup>Δ13</sup> mother and a heterozygous *Igf2P0* father, giving the

genotypes *H19*<sup>Δ13</sup>-*Igf2P0*<sup>-</sup> (*H19*<sup>Δ13</sup>/*Igf2P0* double mutant) and *H19*<sup>-</sup>*Igf2P0*<sup>+</sup> (*H19*<sup>Δ13</sup> single mutant; further information in Supplemental Fig. S1). Pregnant females were killed by cervical dislocation, and the fetuses were dissected at embryonic day (E)16 and E19 (E1 was defined as the day of vaginal plug detection).

### Genotyping

Transmission of the *H19*<sup>Δ13</sup> allele was identified by PCR. The primer pair used to amplify an 895-bp fragment across the deletion was as follows: *H19F*, 5'-TGCCACAGAGGAA-GAAACCAG-3'; *H19R*, 5'-AGTCATAGCCGAATAGCC-3'. A third primer was used as an internal positive control for the PCR reaction amplifying a 494-bp fragment: *H19WT*, 5'-TTCAGTCACTTCCCTCAGCCTC-3'. The transmission of the *Igf2P0* allele was identified by PCR, as described previously (15).

### Placental transport assays of radiolabeled solutes

We performed placental transfer assays according to our previous publications (14, 15). Briefly, radiolabeled solutes were injected into the jugular vein of *H19*<sup>Δ13</sup> females either crossed with C57BL6/J males or heterozygous *Igf2P0* males. Radioactive counts in each fetus were then used to calculate the amount of radioisotope transferred per gram of placenta or per gram of fetus. Average values for WT and mutant fetuses within a litter were then calculated and expressed as a ratio of mutant to WT for that litter. These values could then be used to calculate a mean for all litters at E16 and E19. The fetal accumulation of radioisotope expressed relative to placental weight and plotted as a ratio of mutant to WT gives a relative measure of placental transfer of solute; when expressed relative to fetal weight gives a relative measure of the amount of solute received by the fetus.

### Stereology

Stereological analysis on *H19*<sup>Δ13</sup> placentas from E16 and E9 mice were performed according to Coan *et al.* (25). Briefly, placentas were weighed and hemisected, and corresponding halves were fixed and embedded for generating paraffin wax or resin sections. Measurements were performed using the Computer Assisted Stereology Toolbox (CAST) 2.0 system from Olympus (Ballerup, Denmark). For the analysis of Jz/Lz proportions in *H19*<sup>Δ13</sup>/*Igf2P0* placentas, a simple grid system was employed, and in excess of a total of 700 points/midline placental section was counted. The percentage of points hitting each of the placental component layers was taken as an estimate of the fraction that each layer comprised of the total placenta.

### mRNA expression studies

mRNA expression levels of nutrient transporter genes were analyzed by Northern blotting as described previously (15). *Igf2P0* expression levels were measured using SYBR Green JumpStart *Taq* ReadyMix (Sigma-Aldrich, St. Louis, MO, USA) with the following primers: *Igf2P0F*, 5'-CTTCAGGAAGTACGAAGCGACT-3'; and *Igf2P0R*, 5'-GTGTCGTAGTTCGTTCTCCTCT-3' (which yield a 101-bp PCR product spanning the intron between U1 and U2 exons). Results were normalized against the reference gene *Gapd*, which was measured using the TaqMan Gene Expression Assay Mm99999915\_g1 (Applied Biosystems, Foster City, CA, USA). All qPCR reactions were performed on an ABI 7900HT system (Applied Biosystems), according to the manufacturer's recommendations.

TABLE 1. Fetal and placental weight and fetal-placental weight ratio of  $H19^{\Delta 13}$  and WT mice

Gestational age	Genotype	n	Fetal wet weight (g)	Placental wet weight (g)	Fetal-placental weight ratio
E16	WT	56	0.414 ± 0.011	0.097 ± 0.002	4.363 ± 0.133
	$H19$	51	0.463 ± 0.012	0.126 ± 0.003	3.721 ± 0.101
	$H19$ /WT (%)		112***	130***	85***
	WT	71	1.143 ± 0.016	0.084 ± 0.001	13.766 ± 0.243
E19	$H19$	88	1.410 ± 0.022	0.122 ± 0.001	11.638 ± 0.192
	$H19$ /WT (%)		123***	145***	85***

Values are means ± SE. \*\*\* $P < 0.001$ .

### Statistical analysis

Differences in mRNA expression levels between group means were evaluated by the 2-tailed unpaired  $t$  test. All other data were analyzed by means of 2-way analyses of variance, with “litters” and “genotype” as the two factors. Data are expressed as means ± SE. For data representing radioactive counts, a logarithmic transformation was carried out before statistical analysis. The summary data from these experiments were then represented as ratios, together with 95% confidence limits.

## RESULTS

### Fetal and placental overgrowth in $H19^{\Delta 13}$ mutants

As described previously (19, 20), maternal inheritance of the  $H19^{\Delta 13}$  mutation results in fetal and placental overgrowth. Fetal wet weight was increased in  $H19^{\Delta 13}$  mutants by 12% at E16 and 23% at E19 compared with WT littermates (Table 1). We found that the overgrowth was more pronounced in the placenta at both gestational ages. Accordingly,  $H19^{\Delta 13}$  placental wet weights were increased by 30% at E16 and 45% at E19 compared to WT. As a result of the disproportionate overgrowth of the placenta,  $H19^{\Delta 13}$  mutants demonstrated a decreased fetal-placental weight ratio (85% of WT for both E16 and E19) (Table 1). This relative inefficiency of the large  $H19^{\Delta 13}$  placenta in supporting fetal growth may have either a morphological and/or functional origin.

### Increased surface area for nutrient exchange in the $H19^{\Delta 13}$ placenta

To investigate the possible morphological causes of  $H19^{\Delta 13}$  placental inefficiency, we studied the structural basis of maternal-fetal nutrient transfer using stereological analyses of mutant *vs.* WT littermate placentas. We found that the placental overgrowth in  $H19^{\Delta 13}$  was global, affecting both the labyrinthine zone (Lz) and junctional zone (Jz) (Supplemental Fig. S2 and Table 2). The absolute volumes of the different components of the  $H19^{\Delta 13}$  placenta and WT littermates are summarized in Table 2. The absolute volume of the Lz was significantly increased to 198 and 167% of WT littermate values at E16 and E19, respectively, similar to the increases of 178 and 179% in Jz volume at E16 and E19, respectively. Within the Lz, further measurements were made of the surface area of trophoblast and blood vessels to establish whether the morphology of the transport surface was normal (Table 3). At both gestational ages, expansion of the  $H19^{\Delta 13}$  Lz was associated with significant increases in the volume and surface areas of maternal blood spaces, fetal capillaries, and trophoblast (Tables 2 and 3). The harmonic mean thickness of the  $H19^{\Delta 13}$  Lz exchange barrier did not differ significantly from WT (Table 3). As a result of the increased surface area, the average theoretical diffusing capacity (TDC) in  $H19^{\Delta 13}$  placentas was dramatically increased to 208 and 158% of WT, at E16 and E19, respectively (Table 3). Thus, the changes in morphology of the  $H19^{\Delta 13}$  placenta are unlikely to explain its decreased efficiency.

TABLE 2. Absolute volume of components in the placenta of  $H19^{\Delta 13}$  and WT mice at 2 gestational ages

Component	E16			E19		
	WT	$H19$	$H19$ /WT (%)	WT	$H19$	$H19$ /WT (%)
Placenta	86.19 ± 1.834	148.82 ± 7.028	173***	77.58 ± 2.462	125.30 ± 5.577	162**
Lz	37.29 ± 1.363	73.83 ± 2.562	198***	35.42 ± 0.969	58.98 ± 2.943	167**
Jz	31.26 ± 2.048	55.61 ± 3.027	178**	22.84 ± 1.248	40.80 ± 1.968	179**
Db	16.52 ± 1.909	15.67 ± 4.130	95	18.78 ± 2.058	25.52 ± 1.691	136
Jz/Lz	0.85 ± 0.083	0.76 ± 0.062	89	0.69 ± 0.046	0.68 ± 0.035	99
Trophoblast	22.85 ± 0.414	46.95 ± 2.359	206***	19.12 ± 0.833	32.72 ± 3.068	171*
MBS	8.00 ± 1.112	15.39 ± 1.007	192**	7.99 ± 0.828	14.19 ± 0.651	178**
FC	6.45 ± 0.557	11.49 ± 1.207	178*	8.31 ± 0.946	12.08 ± 1.351	145

Values are mean ± SE volume ( $\text{mm}^3$ );  $n = 6$  from 3 litters/group. Lz, labyrinthine zone or trophoblast; Jz, junctional zone or spongiotrophoblast; Db, decidua basalis; Jz/Lz, ratio of junctional to labyrinthine volume; MBS, maternal blood spaces; FC, fetal capillaries. \* $P < 0.05$ ; \*\* $P < 0.01$ ; \*\*\* $P < 0.001$ .

TABLE 3. Absolute quantities of measurements of Lz vasculature in the placenta of  $H19^{\Delta13}$  and WT mice at 2 gestational ages

Measurement	E16			E19		
	WT	$H19$	$H19/WT$ (%)	WT	$H19$	$H19/WT$ (%)
MBS SA (cm <sup>2</sup> )	18.81 ± 0.374	39.77 ± 3.051	211**	14.16 ± 1.018	25.08 ± 1.405	177**
FC SA (cm <sup>2</sup> )	15.88 ± 1.084	30.97 ± 3.306	195*	16.17 ± 1.110	24.98 ± 1.871	154*
IMT (μm)	4.20 ± 0.187	4.18 ± 0.152	99	3.11 ± 0.148	3.29 ± 0.356	105
TDC (mm <sup>2</sup> ·min <sup>-1</sup> ·kPa <sup>-1</sup> )	7.2 ± 0.3	15.0 ± 1.9	208*	8.6 ± 0.8	13.6 ± 1.6	158*

Values are means ± SE;  $n = 6$  from 3 litters/group. MBS SA, maternal blood space surface area; FC SA, fetal capillary surface area; IMT, labyrinthine interhemal membrane thickness; TDC, theoretical diffusion capacity of the interhemal membrane. \* $P < 0.05$ ; \*\* $P < 0.01$ .

### The $H19^{\Delta13}$ overgrown placenta down-regulates nutrient supply

Despite the observed expansion in volume and surface area of the Lz trophoblast and the increase in TDC of the  $H19^{\Delta13}$  placenta, we found a pronounced reduction in its passive permeability relative to WT controls. The amounts of <sup>14</sup>C-mannitol and <sup>14</sup>C-inulin transferred per gram of placenta were significantly reduced to 65–80% of the WT values at both E16 and E19 (Fig. 1A). This, combined with the larger size of the placenta, resulted in  $H19^{\Delta13}$  mutant fetuses receiving the same actual amount of the solute as WT littermates, except for <sup>14</sup>C-mannitol at E19 (Fig. 1A).

Next, we investigated the capacity of the placenta to transfer nutrients by facilitated diffusion (<sup>14</sup>C-glucose) and active transport (<sup>14</sup>C-MeAIB) *in vivo* in relation to placental expression of the glucose and system A amino acid transporters. We found that transfer of <sup>14</sup>C-glucose was significantly reduced per gram of placenta compared to WT at both gestational ages (Fig. 1B). Accumulation of <sup>14</sup>C-glucose per gram of fetus was significantly reduced in  $H19^{\Delta13}$  mutants, *i.e.*, fetuses were receiving less of the solute than WT. We found that mRNA levels of glucose transporter *Slc2a3* were reduced significantly in  $H19^{\Delta13}$  compared to WT placenta at E16 but not E19 (Fig. 2). There were no significant changes in mRNA levels of the glucose transporter *Slc2a1* at either gestational age. <sup>14</sup>C-MeAIB transfer per gram of placenta was also less in  $H19^{\Delta13}$  mutants than in their WT littermates (Fig. 1B). How-

ever, in contrast to <sup>14</sup>C-glucose, mutant fetuses were receiving an appropriate amount of <sup>14</sup>C-MeAIB for their size. We found that the levels of mRNA of the *Slc38a4* 2 kb isoform were reduced in  $H19^{\Delta13}$  relative to WT placenta at E19 but not at E16 (Fig. 2). None of the other isoforms of the system A amino acid transporters were altered in expression in the  $H19^{\Delta13}$  placenta.

### Feto-placental signaling of nutrient demand in $H19^{\Delta13}/Igf2$ P0 double mutants

Large placentas can, therefore, respond to resource allocation signals and down-regulate the nutrient transfer capacity when placental supply and fetal demand are genetically matched at a high level. To test whether large placentas can respond to fetal-placental signals when the genetic drive for fetal growth is higher than that for placental growth, we aimed to genetically reduce the degree of placental overgrowth. This was achieved by crossing  $H19^{\Delta13}$  homozygous females (−/−) with *Igf2* heterozygous P0 males (+/−) and examining the progeny at E19. Two possible combinations of  $H19^{\Delta13}$  and *Igf2* mRNA expression were represented among the conceptuses:  $H19^{\Delta13}$  single mutant ( $H19^{\Delta13-}Igf2P0^+$ ) and  $H19^{\Delta13}/Igf2P0$  double mutant ( $H19^{\Delta13-}Igf2P0^-$ ; see Supplemental Fig. S1).  $H19^{\Delta13}/Igf2P0$  placentas showed a specific reduction in P0 levels (~65% of  $H19^{\Delta13}$ , Fig. 3A), as expected from the deletion of one active allele. As a result of reducing P0 levels, the  $H19^{\Delta13}/Igf2P0$  double-mutant placentas

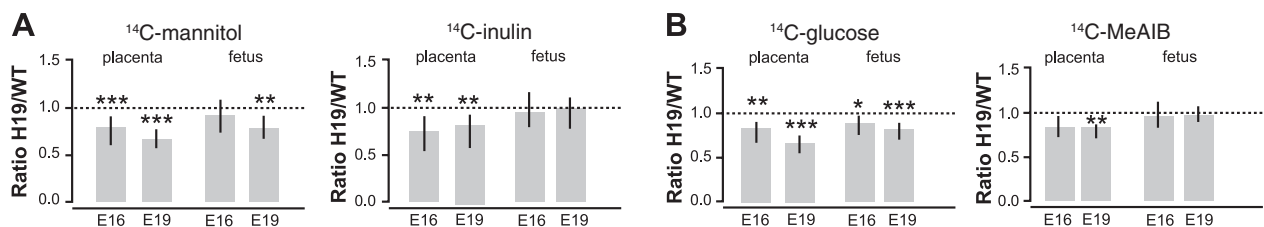


**Figure 1.** Placental transfer of passive diffusion markers, <sup>14</sup>C-mannitol and <sup>14</sup>C-inulin (A) and facilitated and active transport markers, <sup>14</sup>C-glucose and <sup>14</sup>C-MeAIB (B) in  $H19^{\Delta13}$ , calculated as a ratio of mutant to WT transfer, expressed either per gram of placenta or per gram of fetus at 2 gestational ages (E16 and E19). Ratios <1 indicate reduced transfer by the mutant placenta with respect to either placental or fetal weight. (E16: mannitol,  $n=31$   $H19^{\Delta13}$  and  $n=34$  WT from 10 litters; inulin,  $n=30$   $H19^{\Delta13}$  and  $n=28$  WT from 9 litters; MeAIB,  $n=24$   $H19^{\Delta13}$  and  $n=22$  WT from 8 litters; and glucose,  $n=20$   $H19^{\Delta13}$  and  $n=28$  WT from 8 litters. E19: mannitol,  $n=14$   $H19^{\Delta13}$  and  $n=17$  WT from 6 litters; inulin,  $n=63$   $H19^{\Delta13}$  and  $n=71$  WT from 22 litters; MeAIB,  $n=29$   $H19^{\Delta13}$  and  $n=16$  WT from 8 litters; and glucose,  $n=33$   $H19^{\Delta13}$  and  $n=30$  WT from 9 litters.) Bars indicate 95% confidence limits. \* $P < 0.05$ ; \*\* $P < 0.01$ ; \*\*\* $P < 0.001$ .

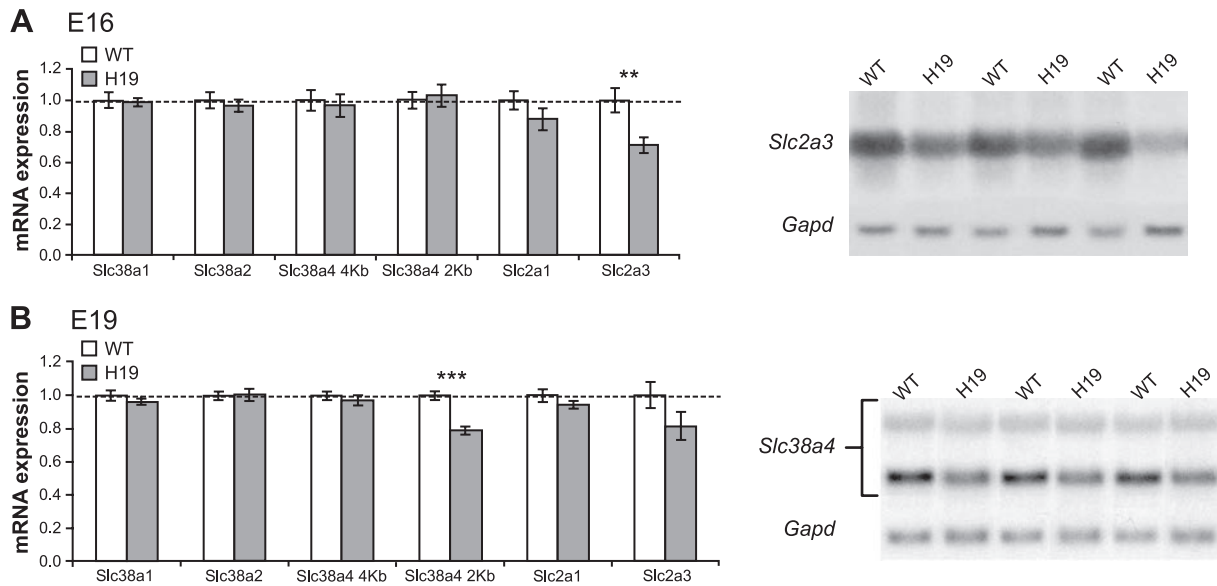


**Figure 2.** Northern blot analysis of mRNA levels of system A amino acid transporter genes *Slc38a1*, *Slc38a2*, and *Slc38a4* and glucose transporter genes *Slc2a1* and *Slc2a3* in *H19 $\Delta$ 13* placentas compared to WT littermates at E16 (A) and E19 (B). Graphs show mean expression levels, with WT levels normalized to 1; Northern blots are representative of total RNA obtained from WT and *H19 $\Delta$ 13* placentas. *Gapd* was used as an internal control for RNA loading (*n* for each genotype and gestational age: *n*=7 for *Slc2a1* and *Slc2a3*; *n*=17 for *Slc38a1* and *Slc38a4*; *n*=10 *Slc38a2*). Bars indicate means  $\pm$  SE. \*\**P* < 0.01; \*\*\**P* < 0.001.

were significantly less overgrown (~15%) than *H19 $\Delta$ 13* single-mutant ( $0.110 \pm 0.001$  g, *n*=80 vs.  $0.130 \pm 0.001$  g, *n*=69, respectively; *P*<0.001) but fetal weights of the *H19 $\Delta$ 13* single and *H19 $\Delta$ 13*/*Igf2P0* double mutants were similar ( $1.370 \pm 0.017$  g, *n*=80 vs.  $1.330 \pm 0.024$  g, *n*=69, respectively; *P*>0.05). The *H19 $\Delta$ 13*/*Igf2P0* double-mutant placenta was thus significantly more efficient compared to *H19 $\Delta$ 13* single-mutant (115% of *H19 $\Delta$ 13*).

Next, we measured maternal-fetal transfer of  $^{14}$ C-MeAIB and  $^{14}$ C-mannitol at E19. We observed increased transfer of  $^{14}$ C-MeAIB per gram in the *H19 $\Delta$ 13*/*Igf2P0* double-mutant placenta as compared with the *H19 $\Delta$ 13* single-mutant (Fig. 3B), which may explain, in part, the relative increase in placental efficiency. No difference in transfer of  $^{14}$ C-mannitol was observed between the genotypes (Fig. 3B). These findings were

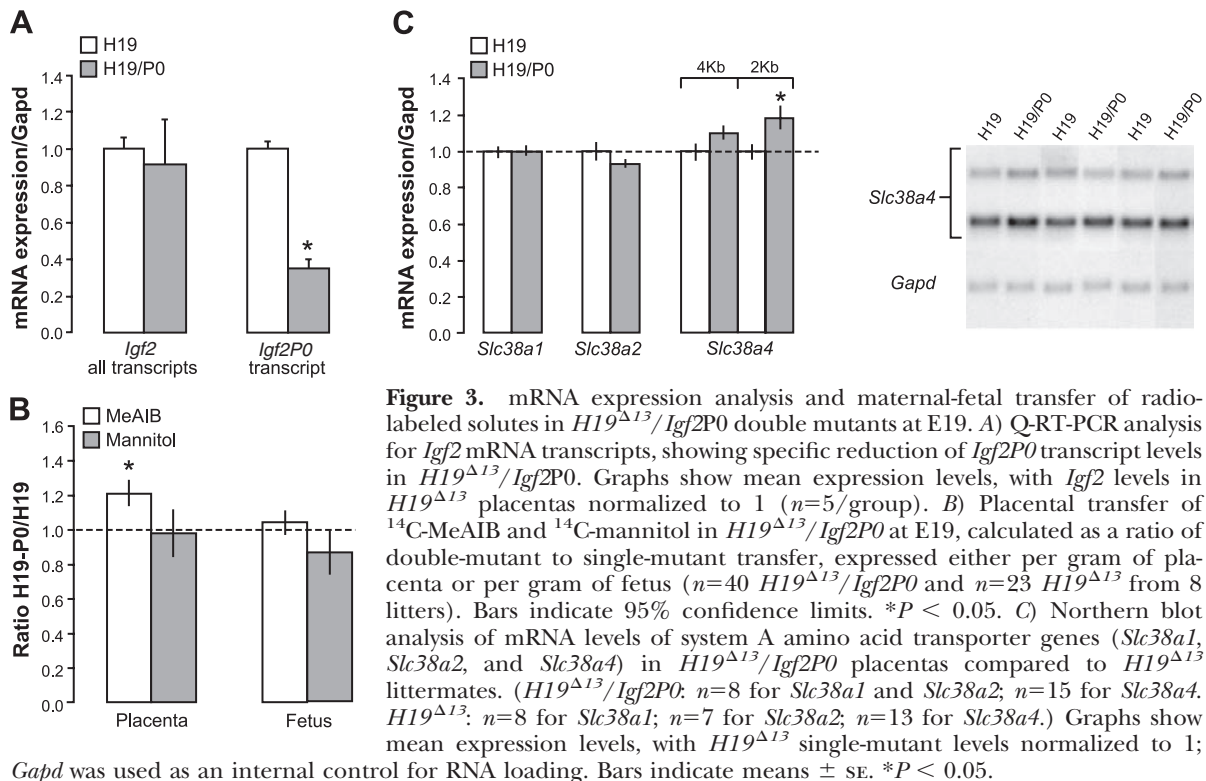


**Figure 3.** mRNA expression analysis and maternal-fetal transfer of radio-labeled solutes in *H19 $\Delta$ 13*/*Igf2P0* double mutants at E19. A) Q-RT-PCR analysis for *Igf2* mRNA transcripts, showing specific reduction of *Igf2P0* transcript levels in *H19 $\Delta$ 13*/*Igf2P0*. Graphs show mean expression levels, with *Igf2* levels in *H19 $\Delta$ 13* placentas normalized to 1 (*n*=5/group). B) Placental transfer of  $^{14}$ C-MeAIB and  $^{14}$ C-mannitol in *H19 $\Delta$ 13*/*Igf2P0* at E19, calculated as a ratio of double-mutant to single-mutant transfer, expressed either per gram of placenta or per gram of fetus (*n*=40 *H19 $\Delta$ 13*/*Igf2P0* and *n*=23 *H19 $\Delta$ 13* from 8 litters). Bars indicate 95% confidence limits. \**P* < 0.05. C) Northern blot analysis of mRNA levels of system A amino acid transporter genes (*Slc38a1*, *Slc38a2*, and *Slc38a4*) in *H19 $\Delta$ 13*/*Igf2P0* placentas compared to *H19 $\Delta$ 13* littermates. (*H19 $\Delta$ 13*/*Igf2P0*: *n*=8 for *Slc38a1* and *Slc38a2*; *n*=15 for *Slc38a4*. *H19 $\Delta$ 13*: *n*=8 for *Slc38a1*; *n*=7 for *Slc38a2*; *n*=13 for *Slc38a4*.) Graphs show mean expression levels, with *H19 $\Delta$ 13* single-mutant levels normalized to 1; *Gapd* was used as an internal control for RNA loading. Bars indicate means  $\pm$  SE. \**P* < 0.05.

not the result of perturbations in the proportions of the Lz and Jz in  $H19^{\Delta13}/Igf2P0$  double-mutant placenta, as these were identical to those in  $H19^{\Delta13}$  single-mutant (Supplemental Fig. S3). We found that transcript levels of system A transporter *Slc38a4* were also modestly increased relative to the  $H19^{\Delta13}$  single mutant (Fig. 3C), which could explain, at least in part, the relative increase in placental transfer of  $^{14}\text{C}$ -MeAIB.

## DISCUSSION

This study, using genetic models of overgrowth and fetal-placental mismatch, provides the first direct evidence that large placentas can modify their nutrient transfer capacity to regulate fetal nutrient acquisition. These adaptations are important to maintain the balance between the fetal genetic drive for growth and the maternal ability to provide these resources, particularly when fetal nutrient demands for growth are high. We have shown that  $H19^{\Delta13}$  placentas, overgrown because of double dosage of *Igf2*, have a reduced passive permeability and transport less glucose and amino acids per gram, despite a greater surface area for nutrient exchange and an increased theoretical diffusion capacity, compared to their WT littermates. This reduction in the nutrient transfer capacity of the large  $H19^{\Delta13}$  single-mutant placenta may limit fetal overgrowth and, thereby, reduce the total demand for maternal nutrients during the period of late pregnancy when the fetus is normally growing most rapidly in absolute terms. Our study also shows that decreasing the overgrowth of the large  $H19^{\Delta13}$  placenta by genetically removing ~65% of the *Igf2* placental-specific P0 transcripts results in relative up-regulation of system A activity and maintenance of fetal overgrowth.

### Placental morphology

Differences in placental morphology do not explain why the fetuses were less overgrown than the placentas in the  $H19^{\Delta13}$  mutants. Genotype had no effect on the volume fractions of the two main placental zones or of the different components within the Lz, the region responsible primarily for nutrient exchange. As a consequence, the surface area for nutrient exchange and the calculated TDC of the  $H19^{\Delta13}$  was 2-fold higher than WT littermates at E16, and > 1.5-fold higher at E19. Thus, the  $H19^{\Delta13}$  large placenta appears morphologically able to support fetal growth well beyond the observed increase in fetal growth. However, the possibility still exists that absolute blood flow or flow matching in the two circulations perfusing the placenta may differ in these large mutants, as a recent report shows that *Igf2* levels affect transcription of several angiogenic factors (26). If hemodynamic alterations occur in the  $H19^{\Delta13}$  large placenta, they would affect most readily the transfer of lipophilic molecules, such as oxygen, rather than hydrophilic molecules using the paracellular route or molecules requiring transporters (27–29).

### Placental transport characteristics

The relative inefficiency of the large  $H19^{\Delta13}$  single-mutant placenta is more likely to be due to the reduced transfer of substances by the three principal mechanisms of transplacental transfer, namely passive diffusion, facilitated diffusion, and active transport. We demonstrated a reduction in transfer of radiolabeled markers of passive diffusion across the  $H19^{\Delta13}$  single-mutant placenta to 65–80% of their WT values at both E16 and E19, despite the increases in Lz surface area and TDC.

Facilitated diffusion of glucose across the  $H19^{\Delta13}$  placentas was also only 63–77% of the WT values per gram of placenta, with the result that the  $H19^{\Delta13}$  fetuses accumulated less glucose per gram of fetal weight. In part, this may result from the diversion of glucose from transplacental transfer to accumulation as placental glycogen within the placenta, as  $H19^{\Delta13}$  placentas are known to have higher glycogen contents than their WT littermates during late gestation (30). At E16, the decreased glucose transfer across the  $H19^{\Delta13}$  placentas may also reflect the reduced expression of the placental glucose transporter *Slc2a3/Glut3*. However, at E19, there were no changes in expression of either placental glucose transporter from WT values, which suggests there may be a simple diffusional component to glucose transfer across the mouse placenta in late gestation. Whatever the mechanisms involved, the decrease in placental glucose delivery per gram of  $H19^{\Delta13}$  fetus will limit its growth relative to the size of its placenta.

Like simple and facilitated diffusion, active transport across the  $H19^{\Delta13}$  mutant placenta, measured as maternal-fetal transfer of MeAIB per gram of placenta, was reduced at both E16 and E19. At E19, this may be related, in part, to the reduced expression levels of the 2-kb transcript of *Slc38a4*, one isoform of the system A family of amino acid transporters known to transfer MeAIB across the placenta (15, 31). However, since the  $H19^{\Delta13}$  Lz was larger, total transfer of MeAIB to the  $H19^{\Delta13}$  fetus still exceeded that of the WT at both ages, although this was less than would be predicted from placental size alone. When placental overgrowth was reduced in the double  $H19^{\Delta13}/Igf2P0$  mutant placenta by decreasing the levels of *Igf2P0* transcripts (Fig. 4), we observed that fetal overgrowth was maintained, at least in part, by up-regulation of placental *Slc38a4* expression and MeAIB transport relative to the single mutant. The volume of the placental component layers remained unchanged in double compared to single mutants, ruling out morphological changes as the cause of the increased efficiency of the double-mutant placenta. Taken together, the findings on the two  $H19^{\Delta13}$  mutants suggest that the large  $H19^{\Delta13}$  placenta adapts its nutrient transfer capacity dynamically to regulate resource allocation to the fetus (see summary of findings in Fig. 4).

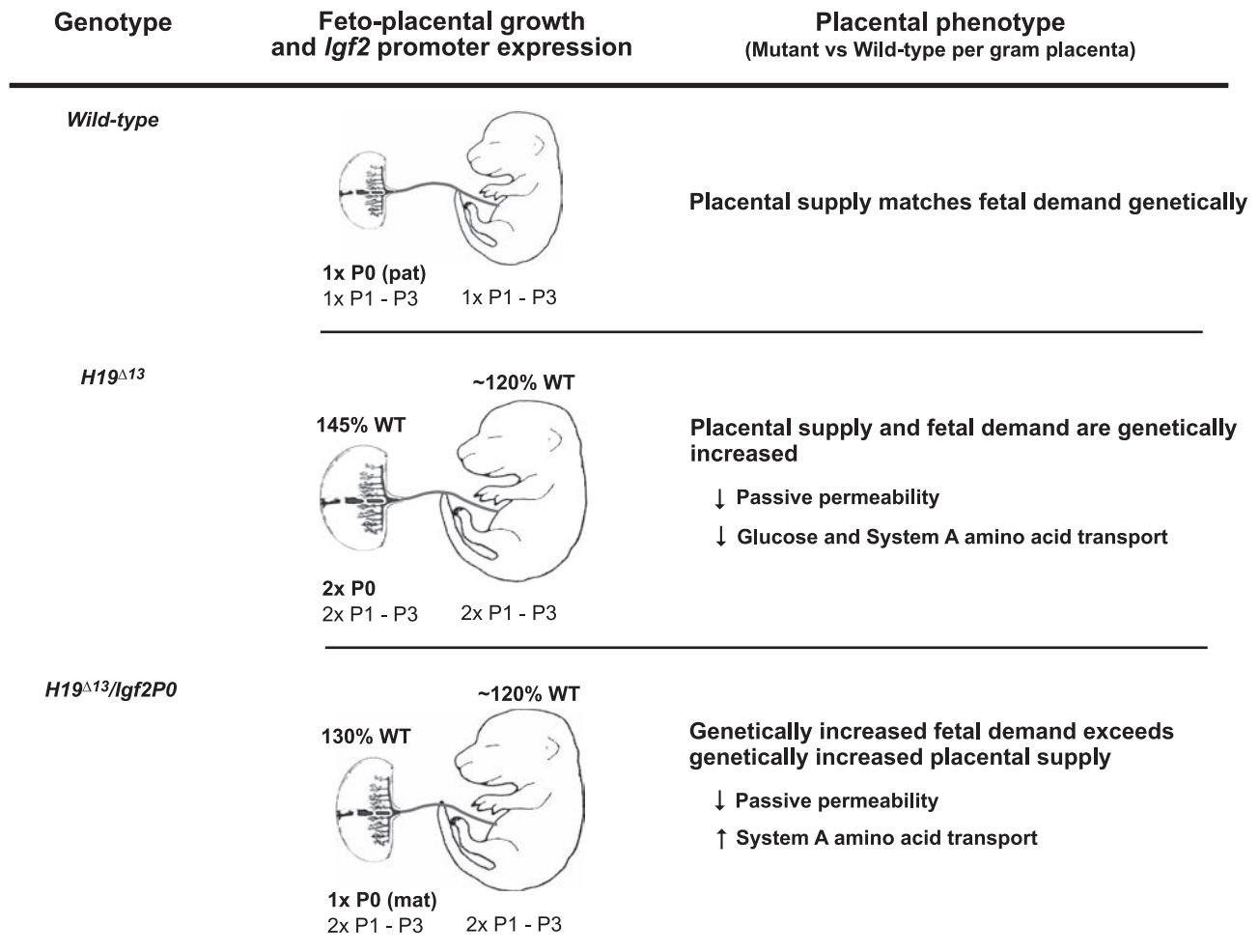


**Figure 4.** Altered balance between fetal and placental growth in  $H19^{\Delta 13}$  and  $H19^{\Delta 13}/Igf2P0$  models of overgrowth. Growth is represented as a percentage of WT littermates (% WT) at E19. Relative levels of *Igf2* promoters (P0-P3) are indicated for each genotype. Levels of the *Igf2* placental-specific isoform P0 determine in part the degree of placental overgrowth and supply potential, whereas fetal *Igf2* P1-P3 determine fetal demand.  $H19^{\Delta 13}$  mutants show disproportionate growth of the placenta relative to the fetus and increased supply-potential relative to fetal demand. However, despite a dramatic increase in surface area for exchange of nutrients associated with overgrowth of the whole placenta, the passive permeability of the placenta and flux of nutrients to the fetus is dramatically reduced per gram of placenta compared to controls. We suggest that this reduction in supply of nutrients is controlled either by growth demand signals emanating from the fetus or by maternal constraint signals. Double  $H19^{\Delta 13}/Igf2P0$  mutants differ from single  $H19^{\Delta 13}$  mutants in that they carry only 1 active copy of the *Igf2* placental-specific P0 allele (the maternal one) instead of 2 (maternal and paternal). Placental overgrowth is thus reduced compared to  $H19^{\Delta 13}$  mutants, with levels of fetal demand unaffected. This reduction in placental supply mediated by loss of the *Igf2* P0 isoform relative to the double mutant results in an adaptive compensatory response, e.g., up-regulation of system A activity, that helps maintain fetal overgrowth. These findings provide the first direct demonstration that overgrown placentas are responsive to fetal-placental signaling of nutrient demand and can adapt their phenotype to control nutrient allocation to the fetus in relation to the balance between maternal nutrient availability and fetal demands for growth.

### Demand signals

The nature of the adaptive signals influencing placental phenotype in the  $H19^{\Delta 13}$  mutants remains unknown but may have a fetal and/or maternal origin. In the  $H19^{\Delta 13}/Igf2P0$  double mutant, the fetal drive for nutrients produced by biallelic expression of all *Igf2* transcripts in the fetus will exceed the supply of nutrient delivered by the less overgrown placenta expressing the *Igf2P0* transcript monoallelically from the normally silent, maternal *Igf2P0* promoter (Fig. 4). The concomitant up-regulation of system A activity in the  $H19^{\Delta 13}/Igf2P0$  placenta is, therefore, likely to be an adaptive

response to a fetal signal of this mismatch designed to help meet the fetal genetic drive for nutrients for growth. Indeed, fetal overgrowth was maintained in the  $H19^{\Delta 13}/Igf2P0$  double mutant despite a 15% reduction in placental weight compared to the single  $H19^{\Delta 13}$  mutant biallelically expressing *Igf2* in all fetal-placental tissues. Similar up-regulation of placental *Slc38a4* expression and MeAIB transport is seen when nutrient demand and supply are mismatched by restricting placental relative to fetal growth in the single *Igf2P0* mutant (15). In the single  $H19^{\Delta 13}$  mutant, down-regulation of placental *Slc2a3* and *Slc38a4* transporters and transfer of glucose and MeAIB may also be a

response to fetal signals designed to reduce the uptake of substrates in line with the reduced passive diffusion of other key substances required for intrauterine growth. Alternatively, maternal signals may be constraining placental nutrient allocation to the large  $H19^{\Delta 13}$  fetuses at the period of late gestation when the absolute demand for nutrients is at its greatest. By reducing expression of key transporters, these maternal signals may place an upper limit on nutrient transfer and avoid excess drainage of maternal resources into fetuses with an increased genetic drive for growth. However, little is known about the maternal metabolic or endocrine environment in these mutants.

### Importance for the human infant

The adaptive regulation of nutrient supply by the large  $H19^{\Delta 13}$  placenta, identified here for the first time, has important implications for our understanding of placental biology and the control of intrauterine growth. Optimal fetal growth is of critical importance to pregnancy outcome, with as many as 15% of all human pregnancies complicated by aberrant fetal growth. The  $H19^{\Delta 13}$  mouse model recapitulates the fetal overgrowth and placentomegaly characteristics of the human disorder Beckwith-Wiedemann syndrome (20–22). Our work showing that placentomegaly is associated with a reduction in nutrient supply in response to constraint signals raises the hypothesis that similar mechanisms may apply to BWS.

Maternal nutrient excess and increased placental nutrient transfer are likely to play causal roles in the development of idiopathic LGA and macrosomic babies arising from maternal or gestational diabetes. Increased transfer of nutrients (*e.g.*, system A and glucose) has been reported in fetal overgrowth in association with fetal macrosomia in human diabetic pregnancy and in mice fed high-fat diets (32–34). The  $H19^{\Delta 13}$  and  $H19^{\Delta 13}/Igf2P0$  mice described in this study are 2 mouse models of genetically determined LGA that differ in their degree of placental overgrowth and show that the trophoblast has an active, dynamic role in the regulation of fetal overgrowth. The absolute and relative amounts of nutrients transferred across overgrown placentas may differ between individual LGA infants with consequences for their morbidity and mortality rates both at birth and much later in life. Although the signals regulating the nutrient supply capacity of the placenta remain unknown, the results of this and our previous studies (15, 18) show that the placenta is responsive to mismatches between nutrient availability and the fetal genetic drive for nutrient acquisition. The placenta is, therefore, acting as a nutrient sensor and adapting its phenotype to optimize the nutrient supply to the fetus with respect to the various nutrient allocation signals. FJ

The authors thank Paul Smith for technical help with the placental transfer assays, E. Walters and Anne Segonds-Pichon for help with the statistical analyses, and Prof. Anne

Ferguson-Smith for advice and discussions. This work was supported by grants from the Biotechnology and Biological Sciences Research Council, FP6 Epigenome Network of Excellence, and the Medical Research Council Center for Obesity and Related Metabolic Disorders.

### REFERENCES

- Zhang, X., Decker, A., Platt, R. W., and Kramer, M. S. (2008) How big is too big? The perinatal consequences of fetal macrosomia. *Am. J. Obstet. Gynecol.* **198**, 517e1–517e6
- Stotland, N. E., Caughey, A. B., Breed, E. M., and Escobar, G. J. (2004) Risk factors and obstetric complications associated with macrosomia. *Int. J. Gynaecol. Obstet.* **87**, 220–226
- Boney, C. M., Verma, A., Tucker, R., and Vohr, B. R. (2005) Metabolic syndrome in childhood: association with birth weight, maternal obesity, and gestational diabetes mellitus. *Pediatrics* **115**, 290–296
- Simeoni, U., and Barker, D. J. (2009) Offspring of diabetic pregnancy: long-term outcomes. *Semin. Fetal Neonatal Med.* **14**, 119–124
- Seidell, J. C. (2000) Obesity, insulin resistance and diabetes—a worldwide epidemic. *Br. J. Nutr.* **83**(Suppl. 1), S5–S8
- Jansson, T., and Powell, T. L. (2006) Human placental transport in altered fetal growth: Does the placenta function as a nutrient sensor?—A review. *Placenta* **27**(Suppl. A), S91–S97
- Jansson, T., and Powell, T. L. (2007) Role of the placenta in fetal programming: underlying mechanisms and potential intervention approaches. *Clin. Sci.* **113**, 1–13
- Fowden, A. L., Sferruzzi-Perri, A. N., Coan, P. M., Constância, M., and Burton, G. J. (2009) Placental efficiency and adaptation: endocrine regulation. *J. Physiol.* **587**, 3459–3472
- Reik, W., Constância, M., Fowden, A. L., Anderson, N., Dean, W., Ferguson-Smith, A. C., Tycko, B., and Sibley, C. P. (2003) Regulation of supply and demand for maternal nutrients in mammals by imprinted genes. *J. Physiol.* **547**, 35–44
- Maher, E. R., and Reik, W. (2000) Beckwith-Wiedemann Syndrome: imprinting in clusters revisited. *J. Clin. Invest.* **105**, 247–252
- Gicquel, C., and Le-Bouc, Y. (2006) Hormonal regulation of fetal growth. *Horm. Res.* **65**(Suppl. 3), 28–33
- Constância, M., Kelsey, G., and Reik, W. (2004) Resourceful imprinting. *Nature* **432**, 53–57
- Tycko, B., and Morison, I. M. (2002) Physiological function of imprinted genes. *J. Cell. Physiol.* **192**, 245–258
- Constância, M., Hemberger, M., Hughes, J., Dean, W., Ferguson-Smith, A. C., Fundele, R., Stewart, F., Kelsey, G., Fowden, A. L., and Reik, W. (2002) Placental-specific IGF-II is a major modulator of placental and fetal growth. *Nature* **417**, 945–948
- Constância, M., Angiolini, E., Sandovici, I., Smith, P., Smith, R., Kelsey, G., Dean, W., Ferguson-Smith, A. C., Sibley, C. P., Reik, W., and Fowden, A. L. (2005) Adaptation of nutrient supply to fetal demand in the mouse involves interaction between the *Igf2* gene and placental transporter systems. *Proc. Natl. Acad. Sci. U. S. A.* **102**, 19219–19224
- Angiolini, E. J., Fowden, A. L., Coan, P., Sandovici, I., Smith, P., Dean, W., Burton, G. J., Tycko, B., Reik, W., Sibley, C. P., and Constância, M. (2006) Regulation of placental efficiency for nutrient transport by imprinted genes. *Placenta* **27**(Suppl. A), S98–S102
- Dilworth, M. R., Kusinski, L. C., Cowley, E., Ward, B. S., Husain, S. M., Constância, M., Sibley, C. P., and Glazier, J. D. (2010) Placental-specific *Igf2* knock-out mice exhibit hypocalcemia and adaptive changes in placental calcium transport. *Proc. Natl. Acad. Sci. U. S. A.* **107**, 3894–3899
- Coan, P. M., Vaughan, O. R., Sekita, Y., Finn, S. L., Burton, G. J., Constância, M., and Fowden, A. L. (2008) Adaptations in placental nutrient transfer capacity to meet fetal growth demands depend on placental size in mice. *J. Physiol.* **586**, 4567–4576
- Leighton, P. A., Ingram, R. S., Eggenschwiler, J., Efstratiadis, A., and Tilghman, S. M. (1995) Disruption of imprinting



- caused by deletion of the *H19* gene region in mice. *Nature* **375**, 34–39
20. Eggenschwiler, J., Ludwig, T., Fisher, P., Leighton, P. A., Tilghman, S. M., and Efstratiadis, A. (1997) Mouse mutant embryos overexpressing IGF-II exhibit phenotypic features of the Beckwith-Wiedemann and Simpson-Golabi-Behmel syndromes. *Genes Dev.* **11**, 3128–3142
  21. Choufani, S., Shuman, C., and Weksberg, R. (2010) Beckwith-Wiedemann Syndrome. *Am. J. Med. Genet. C. Semin. Med. Genet.* **154C**, 343–354
  22. Weng, E. Y., Moeschler, J. B., and Graham, J. M. (1995) Longitudinal observations of 15 children with Wiedemann-Beckwith syndrome. *Am. J. Med. Genet.* **56**, 366–373
  23. Moore, T., Constância, M., Zubair, M., Bailleul, B., Feil, R., Sasaki, H., and Reik, W. (1997) Multiple imprinted sense and antisense transcripts, differential methylation and tandem repeats in a putative imprinting control region upstream of mouse *Igf2*. *Proc. Natl. Acad. Sci. U. S. A.* **94**, 12509–12514
  24. Constância, M., Dean, W., Lopes, S., Moore, T., Kelsey, G., and Reik, W. (2000) Deletion of a silencer element in *Igf2* results in loss of imprinting independent of *H19*. *Nat. Genet.* **26**, 203–206
  25. Coan, P. M., Ferguson-Smith, A. C., and Burton, G. J. (2004) Developmental dynamics of the definitive mouse placenta assessed by stereology. *Biol. Reprod.* **70**, 1806–1813
  26. Kawahara, M., Wu, Q., and Kono, T. (2010) Involvement of insulin-like growth factor 2 in angiogenic factor transcription in bi-maternal mouse conceptuses. *J. Reprod. Dev.* **56**, 79–85
  27. Schröder, H. J. (1995) Comparative aspects of placental exchange functions. *Eur. J. Obstet. Gynecol. Reprod. Biol.* **63**, 81–90
  28. Atkinson, D. E., Boyd, R. D., and Sibley, C. P. (2006) Placental transfer. In: *Knobil and Neill's Physiology of Reproduction* (Neill, J. D., ed.), pp. 2787–2846, Elsevier, London
  29. Fowden, A. L., Ward, J. W., Wooding, F. P. B., Forhead, A. J., and Constância, M. (2006) Programming placental nutrient transport capacity. *J. Physiol.* **572**, 5–15
  30. Esquiliano, D. R., Guo, W., Liang, L., Dikkes, P., and Lopez, M. F. (2009) Placental glycogen stores are increased in mice with *H19* null mutations but not in those with insulin or IGF type 1 receptor mutations. *Placenta* **30**, 693–699
  31. Cramer, S., Beveridge, M., Kilberg, M., and Novak, D. (2002) Physiological importance of system A amino-acid transport to rat fetal development. *Am. J. Physiol. Cell Physiol.* **282**, C153–C160
  32. Jansson, T., Ekstrand, Y., Björn, C., Wennergren, M., and Powell, T. L. (2002) Alterations in the activity of placental amino acid transporters in pregnancies complicated by diabetes. *Diabetes* **51**, 2214–2219
  33. Jansson, T., Cetin, I., Powell, T.L., Desoye, G., Radaelli, T., Ericsson, A., and Sibley, C. P. (2006) Placental transport and metabolism in fetal overgrowth—a workshop report. *Placenta* **27**(Suppl. A), S109–S113
  34. Jones, H. N., Woollett, L. A., Barbour, N., Prasad, P. D., Powell, T. L., and Jansson, T. (2009) High-fat diet before and during pregnancy causes marked up-regulation of placental nutrient transport and fetal overgrowth in C57/BL6 mice. *FASEB J.* **23**, 271–278

*Received for publication October 21, 2010.  
Accepted for publication January 21, 2011.*